FERMI NATIONAL
ACCELERATOR LABORATORIES

Fast Ramping Accelerator Dipole Models for Fermilab's Booster Upgrade and Muon Collider

Technical Division

Supervisor:
Alexander Zlobin
Emanuela Barzi

Intern:
Stefano Mannucci

August-September 2023

Abstract

The future discoveries in the field of High Energy Physics are led by the development of new types of accelerators. Around the world, there are a lot of researchers that are studying some possible designs for the future accelerators and some of them are considering the use of alternating current inside the superconducting magnets in order to have better efficiency. The work described in this report tries to compare some superconducting magnets made of different materials and to understand which one of them can be considered for its better performance working in a variable magnetic field. For this goal, becomes really important to control the temperature of the coil, and, as visible in the next chapter, to relate this parameter to the frequency of the magnetic field, in order to find, as will be named, the *critical frequency*.

Contents

Chapter 1

Introduction

1.1 Accelerator: Muon Colliders and Boosters

There are a lot of types of accelerators under study, all with particular designs and characteristics. For better efficiency and for better performance some of them need fast ramping magnets. This project is taught to analyze magnets that work with alternating current, in some future accelerator as, ad example, the Muon Collider and the Boosters for some synchrotron. The Muon Collider was taught in the last century because muons are interesting leptons that could be used for a new type of accelerator. This particles has some specific characteristic: they have the same charge as the electrons but they are 200 times heavier. The main consequence of this characteristic is that the energy released by bremsstrahlung radiation is decreased by a factor of two billion, which permits the development of a really powerful accelerator but using lower energies. As always happens in engineering, there is an important trade-off: the development of this type of accelerator is slowed down by another characteristic of the particles, in fact, the muons decay in 2.2 microseconds at rest. For that reason, the feasibility of this type of accelerator depends, in particular, on the development of superconducting magnets working with fast ramping with this condition:

- $B_m = 2\ T$: peak to peak amplitude of the magnetic field;
- $f \in [0, 500]\ Hz$: frequency of the magnetic field.

In addition, a Booster is used to increase the energy of the particles before injecting them into the main accelerator. For this type of accelerator is needed, at least:

- $B_m = 0.4\ T$;
- $f \in [15, 20]\ Hz$.

For more information on the Muon Collider can be used the link [10] or [11], or for the booster can be used [12]. For a general perspective on the future development of some accelerator is recommended this book [6].

1.2 Superconductors: state of the arts and future development

The main item of the magnet system is to lead the particle beam in an accelerator. In the past, this was done by normal conductors but since their discovery, the technology of the superconducting magnet has been developed. The main property of this type of magnet system is that the resistivity of these materials goes to zero at very low temperatures, letting to develop very high magnetic fields. The main consequence of using a very high magnetic field is to use particles at really high energy, improving the possibility of making important discoveries. For this type of magnet, there are a lot of very important parameters that have been used in this work as:

- $r = Cu/non - Cu\ ratio$;
- $\lambda = \frac{1}{1+r}$: the superconducting fraction;
- d_f: effective filament diameter, diameter of the superconducting filament;
- ρ_n: matrix resistivity;
- $\rho_e = \rho_n \frac{1+\lambda}{1-\lambda}$: effective transverse resistivity;
- L_p: the filament twist pitch;

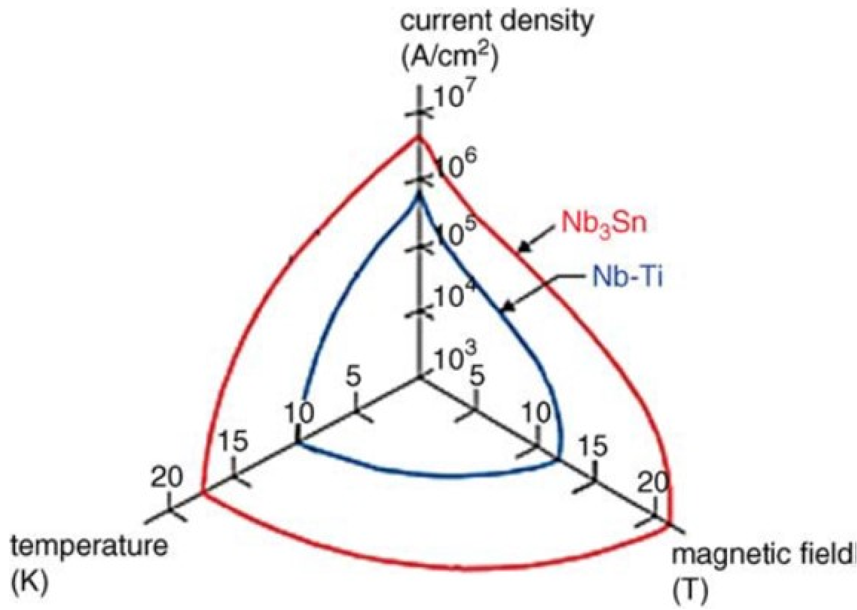

Figure 1.1: Superconducting surface

- $J_c(B, T)$: critical current density of the superconducting magnets;
- $J_e(B, T) = \lambda J_c(B, T)$: engineering current density.

It is important to underline the importance of the critical current density. Using data from the experiment, it is possible to determine the three-dimensional plot of the critical current density for each material. As visible in the figure 1.1 it is possible to define two important parameters of the superconducting magnet:

- T_{c0}: the critical temperature at zero magnetic fields;
- B_{c20}: upper critical magnetic field at zero temperature.

In the following paragraphs, there are described some particular types of superconducting magnets. All the descriptions are taken from the book [1]

1.2.1 $NbTi$

$NbTi$ superconducting magnet has been used during the last decades and is the most used material for the old and current accelerator. Usually, they are made using a copper matrix with the superconducting filaments inside. The technology developed is robust and well-known and so nowadays is a very competitive technology that is limited primarily by the value of the magnetic field that it can reach. In particular:

- $T_{c0} = 9.8\ K$
- $B_{c20} = 14.5\ T$

1.2.2 Nb_3Sn

Nb_3Sn superconducting magnets are the ones that are used for higher magnetic fields with respect to $NbTi$. Usually, they have a bronze or a copper matrix, depending on how they are manufactured. Nowadays they are still in studying and in development, in particular, in the Nuclear Fusion field (for example at the International Thermonuclear Experimental Reactor) or for new accelerators (for example for the Future Circular Collider). This magnets are characterized by:

- $T_{c0} = 18\ K$
- $B_{c20} = 28\ T$

1.2.3 Future development

Today there are under studying a lot of solutions for different types of superconductors. Probably, the most interesting studies include the development of High-Temperature Superconductors, such as the $BSSCO$ or the $YBCO$, characterized by a critical temperature $T_{c0} > 80\ K$ and a critical magnetic field $B_{c20} > 80\ T$ and that can be used to develop a very high magnetic field with relatively high temperature. There are also other studies on different materials as MgB_2 or Nb_3Al, each one characterized by some particular properties. In particular, the MgB_2 cables acquire a lot of interest for this type of application in this project, due to their high critical temperature ($T_{c0} = 38\ K$) and their limited cost.

Chapter 2

The single wire

The first approach that is possible to do is the analysis of a single wire immersed in a homogeneous magnetic field. This work can be considered as the first step before analyzing a dipole. The aim of this work is to find a value of the frequency, in this work called *critical frequency*, at which the magnet changes from a superconducting state to a normal conducting state, with the appearance of additional losses this phenomenon is called *quenching*. To solve this problem became really important to find the energy loss per unit volume and per cycle and to connect that to the temperature of the cable, doing what is called the thermal analyses. There is an important hypothesis that has to be underlined, in fact, the contact resistances between each wire are considered infinite in this work. This hypothesis is made because there are not models in literature in which we can find the contact resistances in rounded cables.

2.1 Modeling the AC Losses

Although in the introduction it is written that the resistances are null in the case of a superconductor, there are some losses in the case of a variable magnetic field. In fact, the changing magnetic field generates a potential difference inside the cable that creates resistance losses. In particular, considering a sample of finite size with an external magnetic field applied H the total loss per unit volume per cycle may be found as:

$$Q = \int H \, dM$$

where M is the magnetization, defined as the total magnetic moment per unit of volume. In this work will be considered two different term, the AC losses due to eddy current and the AC losses due to hysteresis. Solving this problem assumes a big importance in how the magnetic field is applied and, in particular, in this work is considered a fast ramping, as visible in the figure 2.1. In that plot are defined some important quantities as:

- B_m: the magnetic field peak;
- T_m: the time needed to rise at the magnetic field peak.

Can be interesting to see the relation between the frequency and the time of the peak of the magnetic field:

$$f = \frac{1}{2T_m}$$

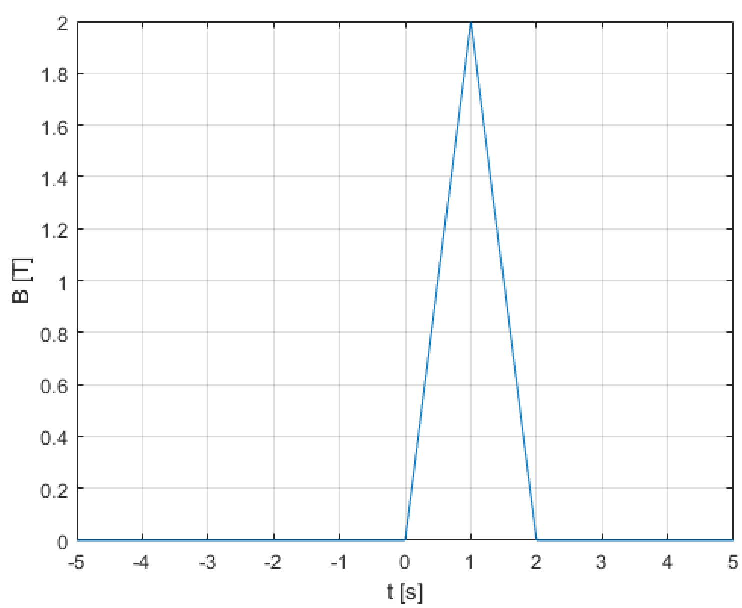

Figure 2.1: Magnetic Field

2.1.1 Eddy Current Losses

The model uses a theory of coupling in twisted composites exposed to a uniform external magnetic field B_e changing at a rate $\dot{B}_e$. With a theoretical part taken from the book [13] it is possible to define a model of the eddy current losses under specific conditions. In this analysis is really important to define the natural time constant of the system τ because the model described in this work is valid only if $\tau << T_m$. The time constant is defined as:

$$\tau = \frac{\mu_0}{2\rho_e}\left(\frac{L_p}{2\pi}\right)^2$$

In which: μ_0 is the magnetic permeability in a vacuum. After some algebra and assuming the external magnetic field equal to the internal magnetic field $\dot{B}_i = \dot{B}_e$ it is possible to define the power losses due to eddy current as

$$P_e = \frac{2\dot{B}_i^{\,2}}{\mu_0}$$

As said before, the critical frequency can be found using the energy losses, which can be calculated as:

$$Q_e(f,T) = 2\int_0^{T_m} P_e(t,f,T)dt \tag{2.1}$$

The factor 2 can be used considering the symmetrical domain in the interval, as visible in the figure 2.1.

2.1.2 Hysteresis Losses

As said before, there is another component of the energy losses that are considered in this work: the hysteresis losses. The analytical solution of a cylinder perpendicular to the magnetic field, which can be easily found in the book [13], is more complicated than the ones for the eddy current losses and, in particular, depends on the penetration of the magnetic field inside the cable. For the practical interest of this work, is possible to neglect this dependency defining the power losses due to hysteresis as

$$P_h = \frac{8}{3\pi} J_c d_f B_m f$$

As done for the eddy current the energy per unit volume and per cycle is:

$$Q_h(f,T) = 2\int_0^{T_m} P_h(t,f,T)dt \tag{2.2}$$

2.2 The Thermal Analysis

The energy developed inside the cable, caused by the losses, has the important consequence to raise the temperature of the cable itself, leading, in the worst situation, to the quenching. For that, the most important thing in this work is to develop a simplified model able to connect the frequency with the temperature inside the cable. Note that in reality, the situation is more difficult than that, and other phenomena, such as the heat deposited from the particle, can compete for the rising of the temperature. To obtain some numerical solution the hypothesis of **adiabatic condition** has been made. At this point, defining the total losses caused by hysteresis and eddy current $Q(f,T) = Q_e(f,T) + Q_h(f,T)$, it is possible to connect the frequency with the temperature using the following energy balance:

$$Q(f,T) = \int_{T_{op}}^{T_{coil}} C_p(T)dT$$

where $C_p(T)$ is the heat capacity. Considering the materials that compose the cables (the matrix and the superconducting material), considering the two different sources of heat and doing some algebra we can expand this formula as:

$$\frac{8}{3\pi}J_e(B,T)d_f B_m + \frac{f(B_m L_p)^2}{\pi^2\rho_e} = \int_{T_{op}}^{T_{coil}} (1-\lambda)C_{p,matrix}(T) + \lambda C_{p,SC}(T)dT \tag{2.3}$$

At this point, the model is completed and can be applied for each type of magnet. In particular, now the problem is to determine all the parameters of each cable, the law of $J_c(B,T)$ and the heat capacity $C_p(T)$.

2.3 Solution

2.3.1 *NbTi*

The first type of superconducting magnets that is studied in this project is a $NbTi$ cables characterized by this geometrical parameters:

- $D = 0.8\ mm$;
- $d_f = 15\ \mu m$;
- $L_p = 40\ mm$;
- $r = 0.5$;
- $\rho_n = 10^{-8}\ \Omega m$

As visible in the equation 2.3 to find the relation between the temperature and the frequency it is needed the critical current density. For this type of superconducting magnet, the critical current density can be obtained from the article [2]. In particular:

$$B_{c2}(T) = B_{c20}\left[1 - \left(\frac{T}{T_{c0}}\right)^{1,7}\right]$$

$$J_c(B,T) = J_{c,ref}\frac{C_0}{B}\left(\frac{B}{B_{c2}(T)}\right)^{\alpha}\left(\frac{B}{B_{c2}(T)}\right)^{\beta}\left[1 - \left(\frac{T}{T_{c0}}\right)^{1,7}\right]^{\gamma}$$

Is possible to see the values of the critical current density at different temperatures and different magnetic fields in the plots 2.2 Using the equation 2.1 and the equation 2.2 is

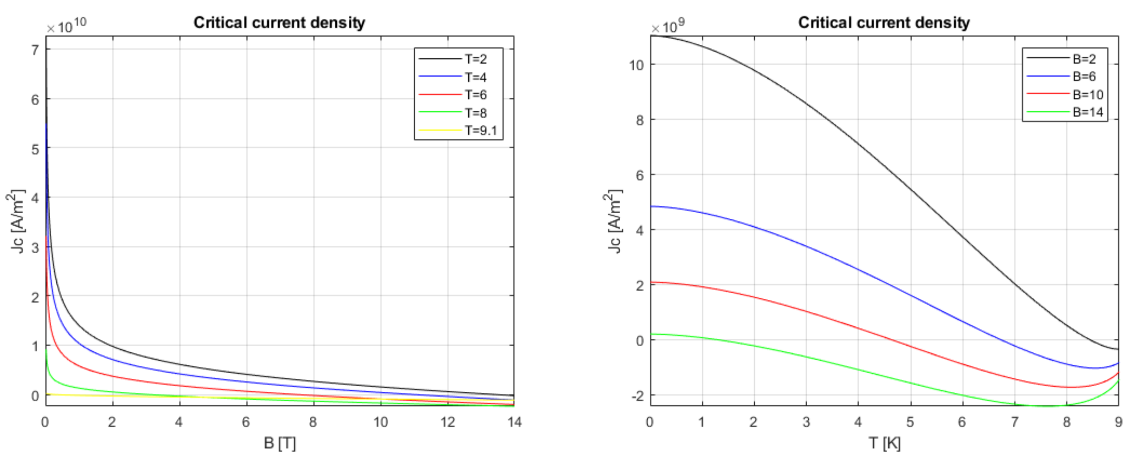

Figure 2.2: Critical Current Density of $NbTi$

possible to obtain the plots of the energy per unit volume and per cycle as visible in figure 2.3. It is interesting to note that the energy per unit volume and per cycle due to eddy current has a linear dependency on the frequency of the magnetic field, instead,

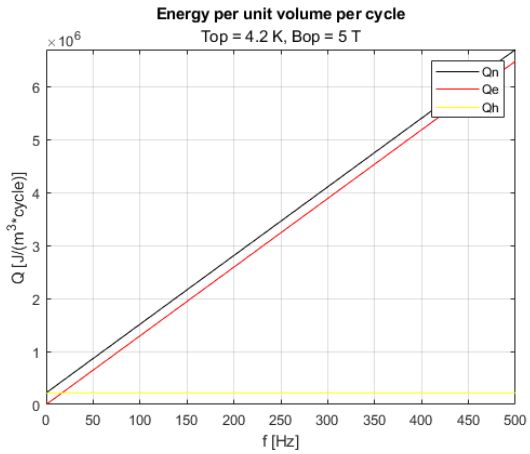

Figure 2.3: Energy per unit volume and per cycle of $NbTi$

the energy due to hysteresis does not depend on the frequency but depends only on the critical current density. This characteristic will be respected by all the magnets. At this point, is possible to obtain the heat capacity of the matrix taking the experimental law from [7] and the heat capacity of the superconductors taking it from [9]. Considering the figure 2.4 the equation 2.3 can be solved by obtaining the critical frequency, as visible from the figure 2.5. Is interesting to see that the Heat Capacity of the $NbTi$ is a function not only of the temperature but it is also a function of the magnetic field and, for that, to solve the equation has been considered a magnetic field of $B = B_{op}$. This condition adds to the solution an approximation and some errors. According to this project and

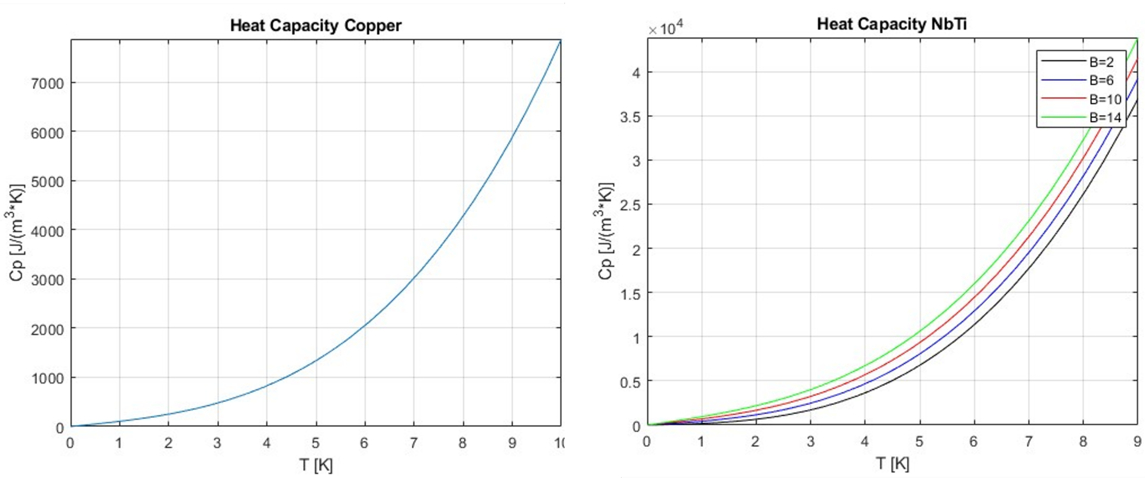

Figure 2.4: Thermal properties of $NbTi$

using the model shown above the critical frequency for this type of cable is $f_{cr} = 5\ Hz$. From the analyses is easy to understand that exist some superconducting magnets that have better performances with respect to this material.

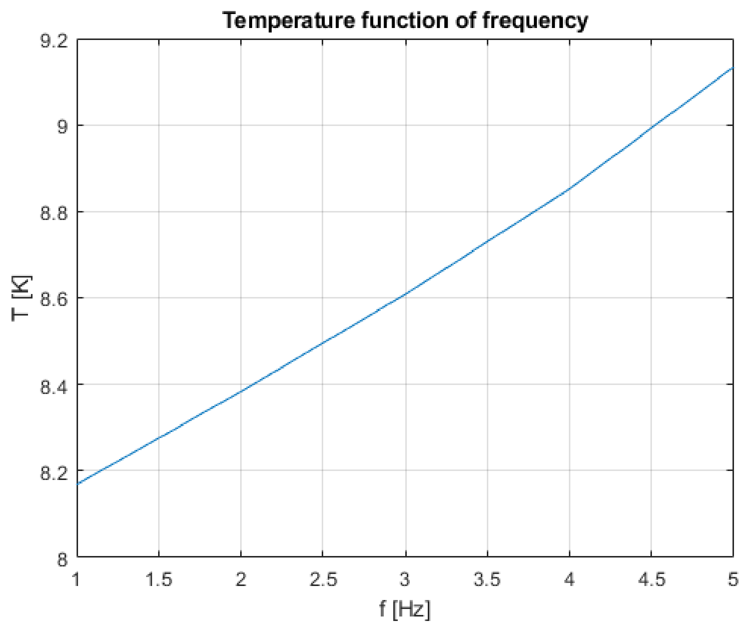

Figure 2.5: Frequency function of temperature of $NbTi$

$NbTi$ **Cu-Ni matrix**

A type of $NbTi$ cable that can be used also for alternating current is characterized by a matrix composed by different material. In fact, in this type, the matrix is made of Cu-Ni with 70% Cu and 30% Ni and the usual used parameters are:

- $D = 1.02\ mm$;
- $d_f = 30\ \mu m$;
- $L_p = 25.4\ mm$;
- $r = 0.18$;
- $\rho_n = 10^{-8}\ \Omega m$

It is possible to do as did before for the $NbTi$ cables, and with exactly the same procedures the final plot of the temperature function of frequency is reached, as visible from the figure 2.6. The thermal properties of nickel can be taken from [8]. It is easy to understand that in this case, the critical frequency is slightly higher than the one of the simple $NbTi$. In fact:

$$f_{cr} = 12\ Hz$$

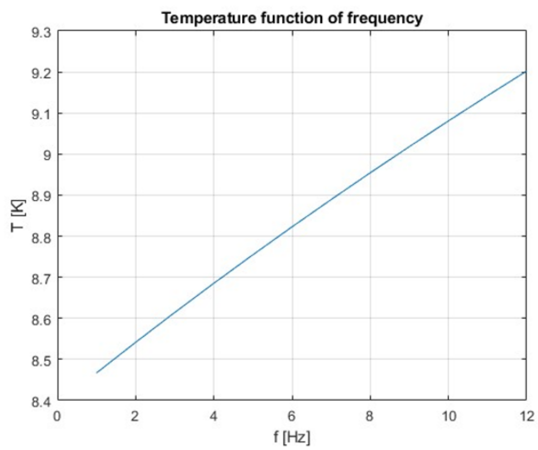

Figure 2.6: Frequency function of temperature for $NbTi$ with Cu-Ni matrix

2.3.2 Nb_3Sn

The third type of superconducting magnet that is studied in this project is a Nb_3Sn cable characterized by these geometrical parameters:

- $D = 0.05\ mm$;
- $d_f = 3\ \mu m$;
- $L_p = 12\ mm$;
- $r = 0.4$;
- $\rho_n = 10^{-8}\ \Omega m$

This cable is a superfine cable that is under study at the **National Institute for Materials Science** in Japan, with the characteristic described in the presentation [4]. This type of superconducting magnet has better behavior with respect to the other two types that are described before. In this case the critical current density can be described with a different formulation that is just a little bit more difficult, obtained again from [2]. J_c is expressed as:

$$T_{c0}(\epsilon) = T_{c0m}\left(1 - a|\epsilon|^{1.7}\right)^{\frac{1}{3}} B_{c2}(T,\epsilon) = B_{c20}(\epsilon)\left[1 - \left(\frac{T}{T_{c0}(\epsilon)}\right)^2\right]$$

$$B_{c2}(T,\epsilon) = B_{c20}(\epsilon)\left[1 - \left(\frac{T}{T_{c0}(\epsilon)}\right)^2\right]$$

$$J_{c(}\epsilon, B, T) = \frac{C(\epsilon)}{\sqrt{B}}\left[1 - \frac{B}{B_{c2}(\epsilon,T)}\right]^2\left[1 - \left(\frac{T}{T_{c0}(\epsilon)}\right)^2\right]^2$$

To obtain some numerical results it is considered the strain $\epsilon = 0$ and the values of the experimental parameter $(a, C(\epsilon)...)$ are used to calibrate the J_c curve with the curve given by the National Institute for Materials Science at $T_{op} = 4.2\ K$. Using all this data and

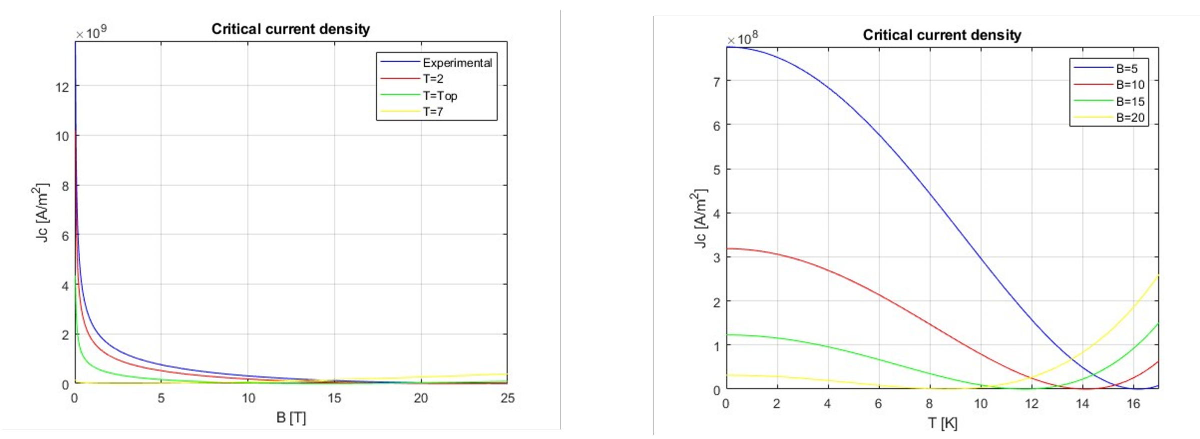

Figure 2.7: Critical Current Density of Nb_3Sn

the model described in the previous paragraphs is possible to obtain the energy per unit volume and per cycle as visible in the figure 2.8. The law of the heat capacity with respect to the temperature of the superconductor and the law of the specific heat of the bronze matrix can be taken from [3] and the plots of the two thermal properties can be seen in the figure 2.9. In conclusion, by solving the usual equation 2.3 it is possible to

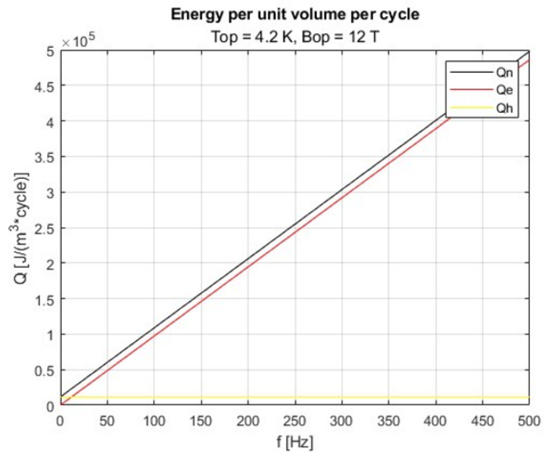

Figure 2.8: Energy per unit volume and per cycle of Nb_3Sn

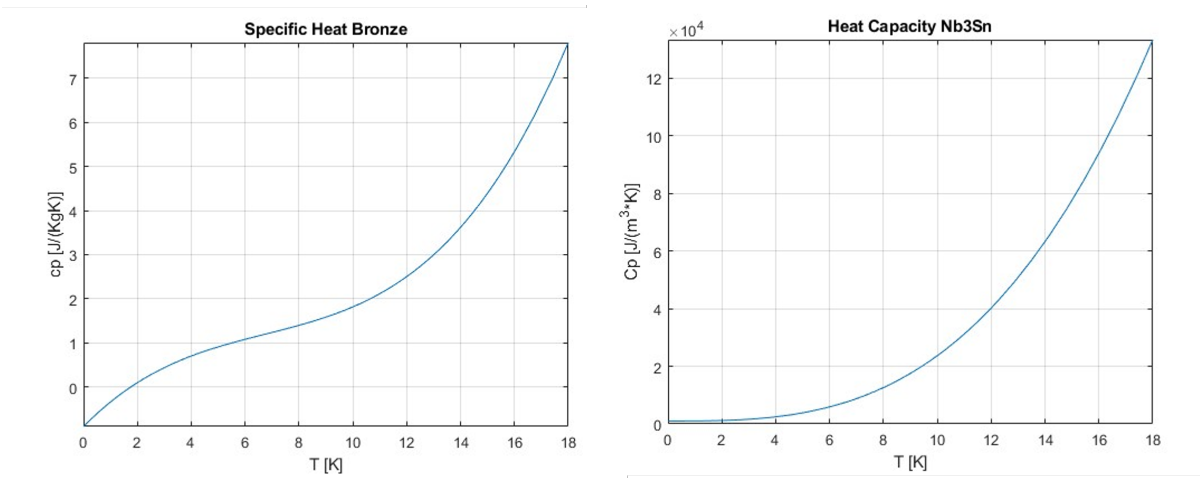

Figure 2.9: Thermal properties of Nb_3Sn cable

obtain the frequency function of the temperature, as visible from the figure 2.10. In this particular case, is easy to understand that this type of superconducting magnet has better performances respect to the other type, with a critical frequency that can reach higher values. In particular, for this cable:

$$f_{cr} = 350\ Hz$$

This value of the critical frequency is really interesting, the Nb_3Sn cable has to be considered and studied for the application in alternating current.

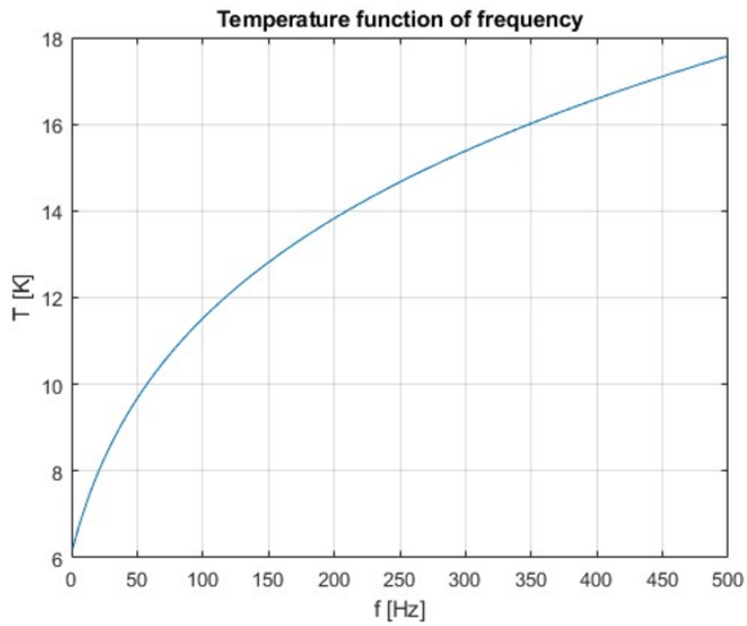

Figure 2.10: Frequency function of temperature for Nb_3Sn

2.3.3 MgB_2

The last type of superconducting magnets under study is the one made of MgB_2. This material is really particular and interesting because, as seen in the first chapter, it has a good balance between critical temperature $T_{c0} = 38\ K$ and the cost of the material. For these reasons, this type of cable is nowadays under study in some laboratories around the world and seems the most promising. As done for the Nb_3Sn in this project are considered some cables with data given from the National Institute for Material Science (visible from [5]). In particular, the following data are considered:

- $D = 0.05\ mm$;
- $d_f = 15\ \mu m$;
- $L_p = 5\ mm$;
- $r = 1$;
- $\rho_n = 10^{-8}\ \Omega m$

The procedure is always the same, but in this case, there is a difference in the critical current density. From the data that are given, it is not possible to determine the dependencies of the critical current density on the temperature so, in first approximation, the critical current density is considered constant with respect to the that parameter. This assumption leads to a solution that probably is too positive, giving some results that are exaggerated. In particular is possible to extrapolate the exponential law of the critical current density from the data taken from the conference [5], as visible from the figure 2.11 The thermal properties of the matrix, which in this case is made of MONEL, a particular

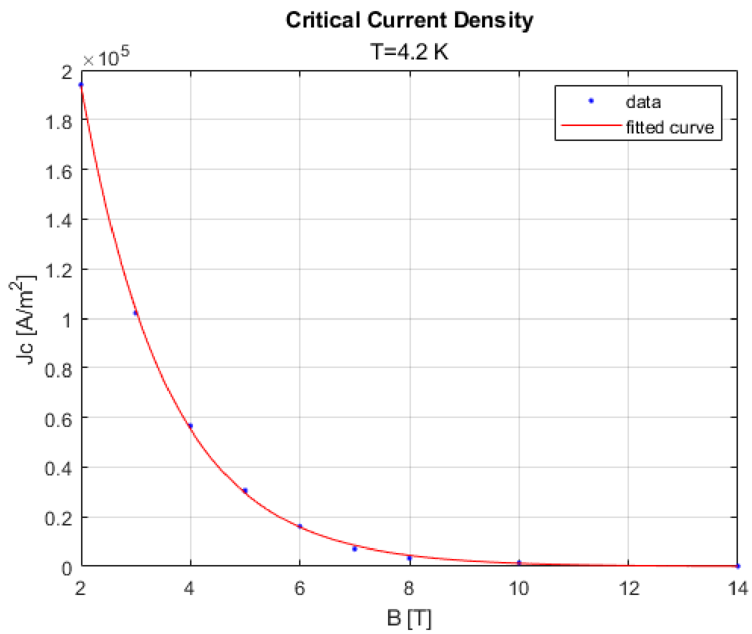

Figure 2.11: Critical Current Density of MgB_2

alloy of copper and nickel, are not known exactly. To have an estimate of his performance is consider the stoichiometric composition of the two main components of this material characterized by more or less 35% Cu and 65% Ni. In particular, taking the specific heat of the copper from [7] and the specific heat of the Nickel from [8] and weighting their value to the composition can be plotted the figure 2.12. The thermal properties of the MgB_2 can be extrapolated from the article [**MgB2**], obtaining the second figure 2.12. The energy per unit volume and per cycle can be calculated (figure 2.13) and the solution of the equation 2.3 can be obtained. Thanks to the higher value of the critical

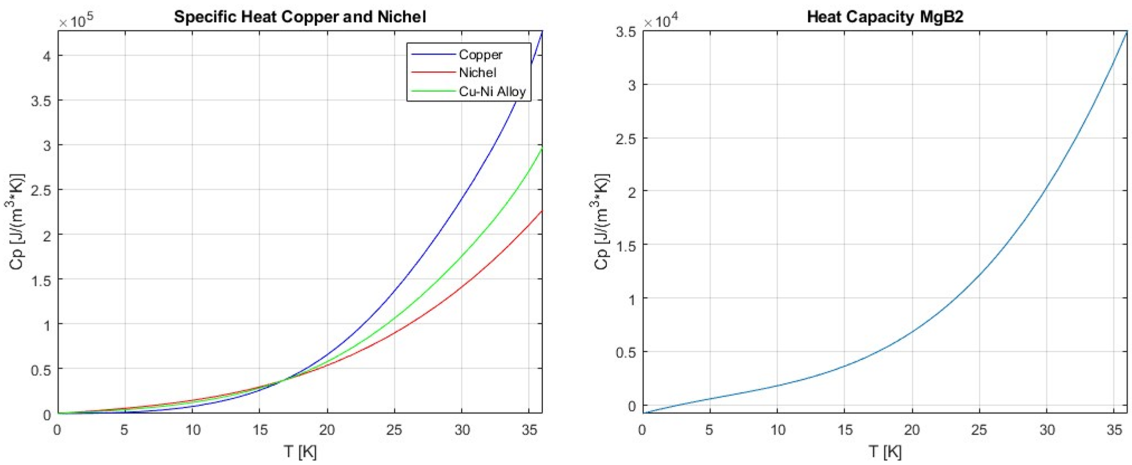

Figure 2.12: Thermal properties of MgB_2 cable

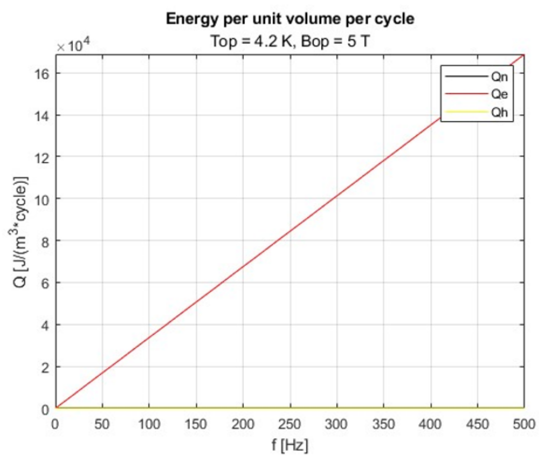

Figure 2.13: Energy per unit volume and per cycle of MgB_2

temperature the critical frequency is really high, in particular:

$$f_{cr} > 4000\ Hz$$

but as said before, this value can be nonphysical. Nevertheless, the model can be corrected obtaining some results that are more physical. From figure 2.14 is visible the relation between the temperature and the frequency also in this case. Considering the results obtained, even if this for sure is exaggerated, this type of superconducting magnet seems to be the best choice in the case of a variable magnetic field. For that reason, there could be some future development of these studies, and will be important to analyze the real behavior of the magnet with some experiments. If the results obtained from this

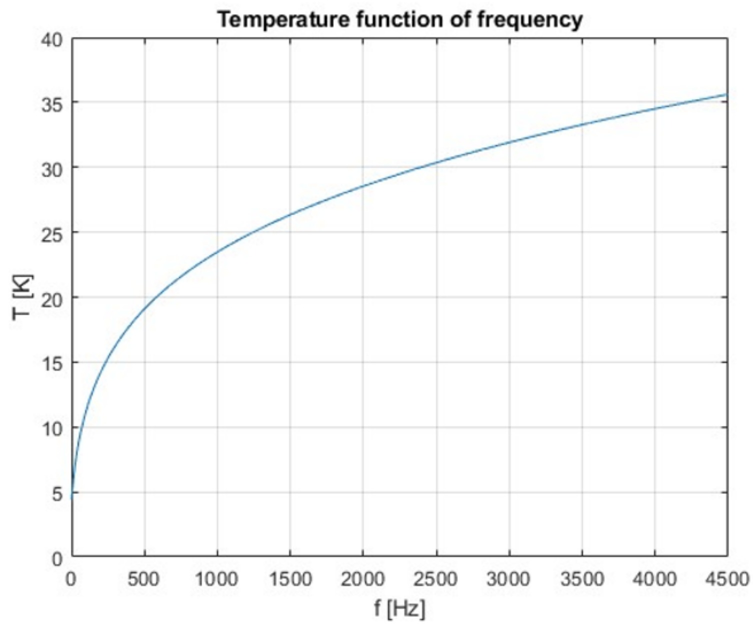

Figure 2.14: Frequency function of temperature for MgB_2

study are correct, the MgB_2 cable will be the best choice for this type of application, at least from this point of view. The results taken are obviously a consequence of the characteristic of this material and in particular, are a consequence of the high value of the critical temperature.

Chapter 3

The Dipole

In the cases studied in the previous chapter is considered only some cables in a constant magnetic field. In this chapter there is described one possible method to apply the model described before and used for the single cable to an entire dipole. In fact, if all the turns of a dipole are divided into small pieces, each of them can be considered as subjected to a uniform external magnetic field. By doing that, it is possible to apply the model of the single wire for each piece and to estimate two interesting results. The first is the total energy developed inside the dipole, which can be important information for the design of the cryogenic system, the second is the critical frequency of the dipole. In particular, this can be taken from the turn subjected to the maximum magnetic field, that result to be the most suffering. Three different cases have been studied during this work, as visible in the figure 3.1. The model has been applied for all three cases but, in this report, only

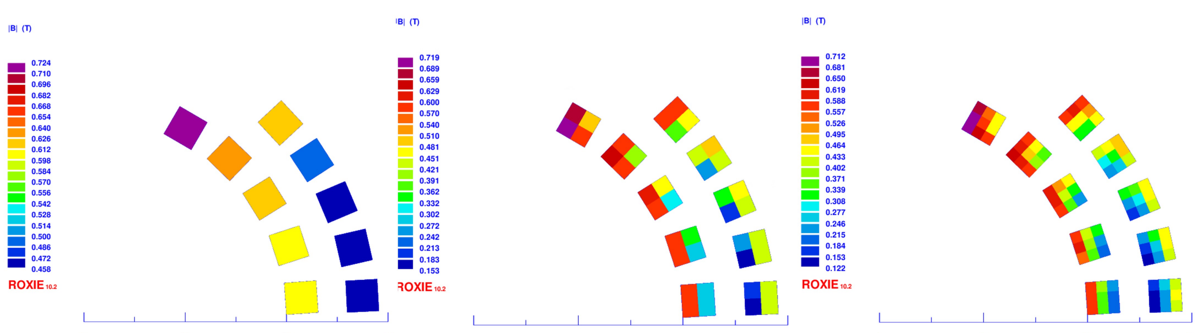

Figure 3.1: Example of some approach for the dipole

the results of the third case are described, being the most conservative and having the most accurate results. Solving the equation 2.3 for each small piece in which the turn is divided is possible to find the solution for all the types of superconducting magnets. To solve the equation the law of the magnetic has to be known, in particular is considered:

$$B_i = \frac{B_i(I)}{I} I(t) \tag{3.1}$$

where $I = 2000\ A$, $I(t)$ come from the law of the alternating current and i indicates the i-th part in which the turn is divided. The results are taken with a current $I(t)$ that has a shape similar to the magnetic field in figure 2.1.

3.1 $NbTi$ dipole

The results show a behavior that is similar to the case of the single wire in a constant magnetic field, the dependencies are exactly the same and the solutions are similar. For this analysis is considered a six-around-one cable made of $NbTi$

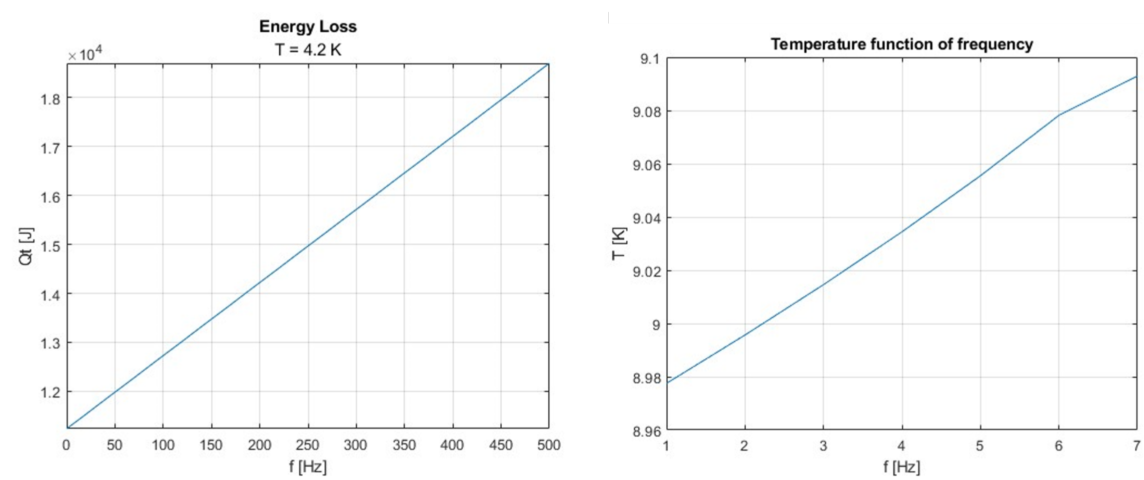

Figure 3.2: Total energy dissipated and frequency function of temperature for $NbTi$ dipole

$$f_{cr} = 7\ Hz$$

3.2 Nb_3Sn dipole

The solution of the Nb_3Sn is slightly different from the case of the single wire, in particular the critical frequency increase. Has to be underlined that the two values cannot be compared, in particular considering that the magnetic field is different in the two cases. However, the solution are visible in the figure 3.3. and the value of the critical frequency is:

$$f_{cr} = 550\ Hz$$

This type of dipole is considered a cable characterized by three levels:

- $N_1 = 36$: Strand Primary Cable;
- $N_2 = 7$: Strand Secondary Cable;
- $N_3 = 7$; Strand Tertiary Cable

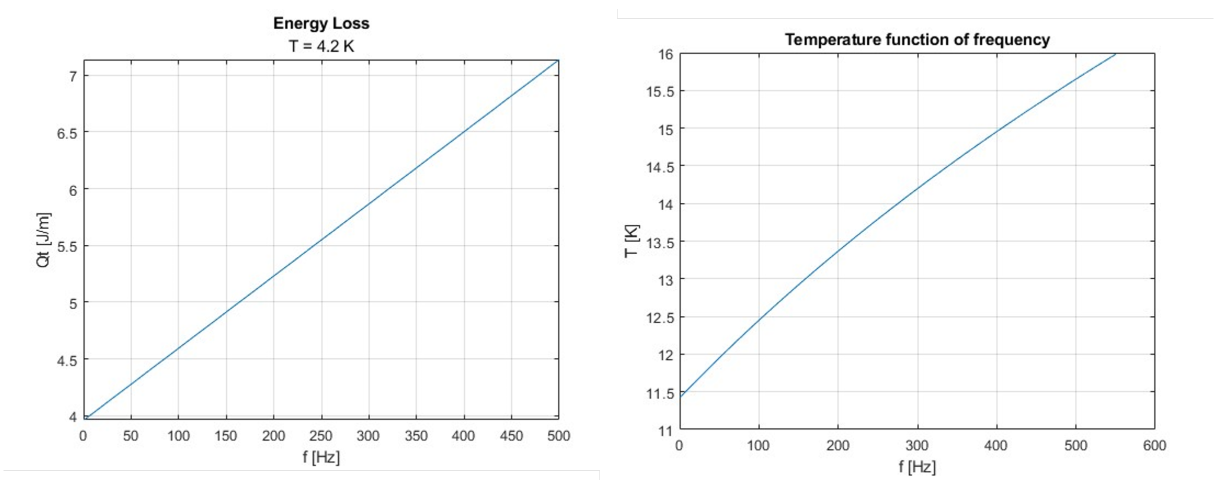

Figure 3.3: Total energy dissipated and frequency function of temperature fo Nb_3Sn dipole

3.3 MgB_2

The last solution can be seen in the figure 3.4. In this case the critical frequency is:

$$f_{cr} > 5000\ Hz$$

and is considered a six-around-one cable.

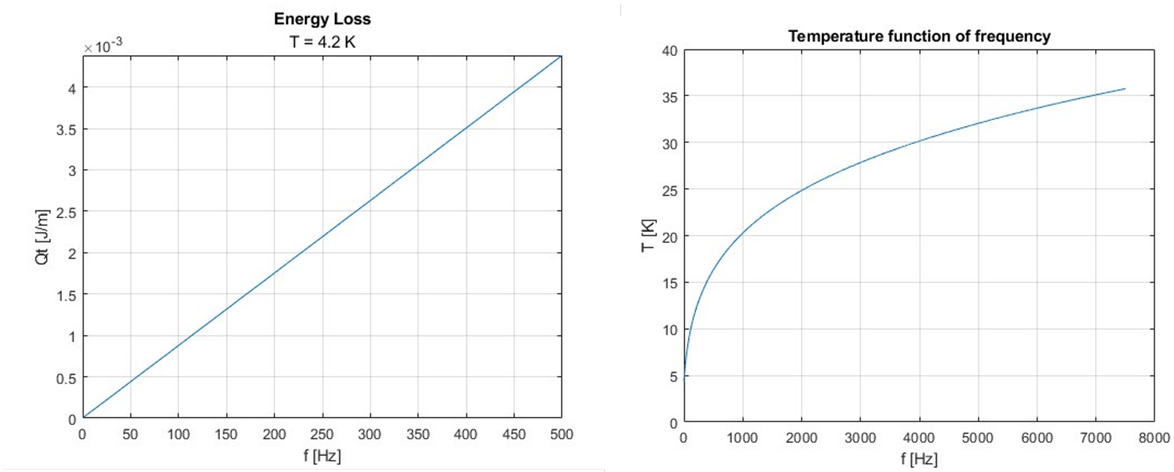

Figure 3.4: Total energy dissipated and frequency function of temperature for MgB_2 dipole

Chapter 4

Conclusion

	$NbTi$	$NbTi$ **Cu-Ni matrix**	Nb_3Sn	MgB_2
f_{cr}: **single cable with** $B_m = 2\ T$	5 Hz	12 Hz	350 Hz	4500 Hz
f_{cr}: **dipole with** $I = 2000\ A$	7 Hz	-	550 Hz	7500 Hz

Table 4.1: Critical Frequencies

This work can be considered as a preliminary work for future studies on this types of material, in particular, the theoretical results obtained can be developed and studied more. The process described is quite easy and simplified, with a lot of assumptions described inside the work, but, even if the results that are obtained can be considered approximate, the success in finding the critical frequency of some different superconducting magnets has to be underlined, as visible all the results are collected in the table 4.1. As visible from Chapter 2 and Chapter 3, what comes out from this work is that the materials that have to be studied for future development of superconducting magnets working in alternating current are the Nb_3Sn and in particular the MgB_2. These two types of superconducting magnets become really interesting considering their critical frequencies, which seem to be really high and could be interesting for future development. For sure, there are at least two things that have to be checked: firstly this project can be improved by developing some models that are more correct, for example, having more experimental data or using the most general formulas for each type of magnet, and secondarily, developing some experiments that can be used to test and verify this model. Considering the first point, for example, during the work is possible to see that the solutions of the $NbTi$ are obtained by removing the dependency on the magnetic field of the heat capacity, or that the solution of the MgB_2 is obtained by removing the dependency on the temperature of the critical current density, and so, for these reasons are expected some errors and, the results obtained for the MgB_2 are too optimistic. At least, there is also one other thing that has to be verified, these cables, for example, have to be studied from a mechanical point of view, verifying if they can really withstand this type of fast ramping. Nevertheless, a lot of work can be done after this project and a lot of interesting topic have been popped up. For that, this report can be considered primarily a first step toward future studies on superconducting magnets working with alternating current.

Appendix A

Building a Magnet

One of the tasks of this project was also to acquire knowledge of the magnets also from a "practical" point of view. The most important success of this part was the building of a model of a magnet, characterized by a classical six-around-one copper cable with a plastic support. As visible from figure A.1, this work was developed in the laboratories of the department and was interesting and really challenging. After some hours of working,

Figure A.1: Building the magnet

and with the teaching of some technicians the final result was achieved, as visible in the figure A.2. This work has been useful firstly for learning how to wind a cable, secondarily to learn all the parts that compose a cable and tertiary to see if the plastic support was a good model for future magnets.

Figure A.2: The final magnet

Bibliography

[1] D. Scherling A. Zlobin. $Nb_3Sn\ Accelerator\ Magnets : Design, Technology\ and\ Performance$. Springer, 2019.

[2] E. Barzi. "Error analyses of short sample, Jc measurement at the short sample facilities". In: ().

[3] A. Davies. "Material properties data for heat transfer modeling in $\mathrm{Nb}_3 Sn\ magnets$". In: ().

[4] A. Kikuchi E. Barzi. "High heat capacity and radiation-resistant organic resins for impregnation of high field superconducting magnets". In.

[5] A. Kikuchi. "EUCAS 2023". In.

[6] N. Mounet. *European Strategy for Particle Physics Accelerator RD Roadmap*. Cern, 2022.

[7] R. P. Reed N. J. Simon E. S. Drexler. *Properties of Copper and Copper Alloys at Cryogenic Temperature*. U.S. Department of Commerce: National Institute of Standards and Technology.

[8] W. F. Glauque R. H. Busy. "The Heat Capacity of Nickel from 15 to 300°K. Entropy and Free Energy Functions". In: ().

[9] L. Dresner S.A. Elrod J.R. Miller. *The Specific Heat of NbTi from 0 to 7 T Between 4.2 and 20 K*. Springer, 1982.

[10] Cern website. URL: `https://home.cern/science/accelerators/muon-collider`.

[11] Fermilab website. URL: `https://www.fnal.gov/muoncollider/`.

[12] Fermilab website. URL: https://www.fnal.gov/pub/science/particle-accelerators/accelerator-complex.html.

[13] M. N. Wilson. *Superconducting Magnets*. Oxford University Press, 1987.